ORIGINAL RESEARCH

Carotid Atherosclerotic Plaque Progression and Change in Plaque Composition Over Time: A 5-Year Follow-Up Study Using Serial CT Angiography

M.J. van Gils
D. Vukadinovic
A.C. van Dijk
D.W.J. Dippel
W.J. Niessen
A. van der Lugt

BACKGROUND AND PURPOSE: Serial in vivo imaging of atherosclerosis is important for understanding plaque progression and is potentially useful in predicting cardiovascular events and monitoring treatment efficacy. This prospective study aims to quantify temporal changes in carotid atherosclerotic plaque volume and plaque composition using MDCTA.

MATERIALS AND METHODS: In 109 patients with TIA or ischemic stroke, serial MDCTA of the carotid arteries was performed after 5.3 ± 0.7 years. The carotid bifurcation was semiautomatically registered for paired baseline follow-up datasets. Outer vessel wall and lumen boundaries were defined using semiautomated segmentation tools. Plaque component volumes were measured using HU thresholds. Annual changes in plaque volume and plaque component proportions were calculated.

RESULTS: One-hundred-ninety-three carotid arteries were analyzed. Plaque volume decreased in 31% and increased in 69% of vessels (range −5.6–10.1%/year). Overall, plaque volume increased 1.2% per year (95% CI, 0.8–1.6, $P \leq .001$). Plaque composition changed significantly from BL (fibrous 66.4%, lipid 28.8%, calcifications 4.8%): fibrous tissue decreased by 1.5%, lipid decreased by 1.8%, and calcification increased by 3.3% ($P < .001$). Intraobserver reproducibility of all volume and proportion measurements was good (ICC 0.78–1.00) and interobserver reproducibility was moderate (ICC 0.76–0.99).

CONCLUSIONS: Changes in carotid plaque burden and plaque composition can be quantified by using serial MDCTA. Plaque burden development is a heterogeneous and slow process.

ABBREVIATIONS: BL = baseline; CCA = common carotid artery; CLL = central lumen line; CoV = coefficient of variation; ECA = external carotid artery; FU = follow-up; HU = Hounsfield unit; ICC = intraclass correlation coefficient; IQR = interquartile range; MDCTA = multidetector CT angiography

Atherosclerosis is a slowly progressing disease, subclinical for decades before suddenly causing clinical manifestations such as coronary artery disease, ischemic cerebrovascular disease, and peripheral artery disease. Increased atherosclerotic burden first causes outward remodeling of the artery, with compensatory expansion of the outer vessel wall boundary without narrowing of the lumen.[1] In later stages of plaque progression, the compensatory mechanism of outward remodeling no longer suffices, and the vessel lumen becomes compromised, eventually causing stenosis or occlusion. Besides the hemodynamic effects on blood flow and blood pressure, atherosclerotic disease is thought to induce ischemic events by plaque rupture, causing thrombosis and obstruction, or thromboembolization, into distal arteries. Increased lipid content, large lipid-rich necrotic cores, intraplaque hemorrhage, inflammation, and thin fibrous caps are the hallmarks of plaques vulnerable to rupture.[2,3]

Knowledge of atherosclerotic plaque development has predominantly been derived from animal and histopathologic studies.[4] Still, little is known about progression of atherosclerosis in humans. Serial in vivo imaging of both vessel lumen and plaque is important for understanding the development of atherosclerotic plaque and its progression from subclinical lesions into rupture-prone plaques. Accurate monitoring of changes in atherosclerotic plaque burden and composition can potentially be used in risk prediction and in assessing efficacy of pharmaceutical treatment.

MDCTA has been validated for imaging atherosclerotic plaque in the carotid arteries in vivo.[5,6] Plaque volume and several plaque components, such as calcifications, lipids, and fibrous tissues, can be accurately quantified.[5,7] MDCTA therefore provides a minimally invasive tool to investigate carotid plaque progression in humans.

In this prospective study, serial CT angiography of the carotid arteries was performed in patients with TIA or ischemic

Received September 2, 2011; accepted after revision October 29, 2011.

From the Departments of Radiology (M.J.v.G., D.V., A.C.v.D., W.J.N., A.v.d.L.), Medical Informatics (D.V., W.Y.N.), Neurology (D.W.J.D.), Erasmus MC University Medical Center, Rotterdam, the Netherlands, and Faculty of Applied Sciences (W.J.N.), Delft University of Technology, Delft, the Netherlands.

This work was supported by a grant from the Netherlands Heart Foundation (2007B161).

Previously presented in part at: Annual Meeting of the Radiological Society of North America, November 26–December 2, 2011; Chicago, Illinois.

Please address correspondence to Aad van der Lugt, MD, PhD, Department of Radiology, Erasmus MC, University Medical Center Rotterdam, Gravendijkwal 230, 3015 CE Rotterdam, the Netherlands; e-mail: a.vanderlugt@erasmusmc.nl

http://dx.doi.org/10.3174/ajnr.A2970

stroke, and changes in plaque burden and plaque composition were quantified using a semiautomated custom-made plaque segmentation tool.

Materials and Methods

Study Population

Patients were recruited from a cohort of 914 consecutive patients with TIA or ischemic stroke who had undergone a standard clinical work-up, including multidetector CT angiography of the carotid arteries.[8] All patients with atherosclerotic plaque (ie, thickening and/or calcification of the vessel wall) in 1 or both carotid arteries were invited to participate in this serial imaging study. Exclusion criteria included no atherosclerotic plaque(s) present at the level of the carotid bifurcation, bilateral occlusion and/or treatment of the carotid arteries, no informed consent, renal insufficiency or hyperthyroidism, and bad image quality of the baseline scan. Blood samples to determine renal function were taken, if necessary. The study was approved by the Local Institutional Ethics Review Board. All patients gave written informed consent.

The serial MDCTA datasets of the first 113 patients included in this study were used for analysis. The MDCTA data from 4 patients were excluded because of motion artifacts or low lumen contrast attenuation. In addition, 6 arteries were excluded from the analysis because of occlusion on baseline and/or follow-up scan; 14 because of local treatment with carotid endarterectomy or stent placement; and 5 because of (focal) poor image quality (perivenous artifacts or streak artifacts due to dental material) impeding correct plaque segmentation. In total, 193 carotid arteries from 109 patients were included in this study.

Clinical Data

As a part of routine clinical work-up, all patients underwent a detailed health questionnaire, a physical examination, laboratory measurements, a CT scan of the brain, and multidetector CT angiography of the carotid arteries. Information was collected on age, sex, medication use, hypertension, hypercholesterolemia, diabetes mellitus, smoking, and history of cerebrovascular or cardiovascular disease, as previously described.[8] During the visit for the follow-up MDCTA scan, a detailed health questionnaire was taken.

Multidetector CT Angiography Protocol

BL scans were performed on a 16- or 64-section multidetector CT scanner (Sensation 16/64; Siemens Medical Solutions, Erlangen, Germany), with a standardized optimized contrast-enhanced protocol (collimation 16×0.75 mm [$n = 106$] or $2 \times 32 \times 0.6$ mm [$n = 3$], pitch 1) and a scan range ranging from the ascending aorta to the intracranial arteries. The follow-up scans were performed on a 128-section multidetector CT scanner (Somatom Definition; Siemens Medical Solutions), with a comparable protocol (collimation $2 \times 64 \times 0.6$ mm, pitch 0.7) and a scan range of 6 cm around the carotid bifurcation. Eighty mL of contrast material was used, with a saline bolus chaser of 40 mL and real-time bolus tracking in the ascending aorta, using a threshold of 120 HU.

Image reconstructions for all scans were made with a FOV of 120 mm, matrix size 512×512, section thickness of 1.0 mm, increment of 0.6 mm, and with both a smooth (B30/B31) and an intermediate (B46) filter kernel, of which the last one has been demonstrated to give the best soft tissue contrast.[9] We performed a point-spread-function analysis using a standard thin wire phantom[10] to test for differences in in-plane resolution between similar kernels on different scanners, but we did not find any differences.

Registration of Baseline and Follow-Up Scan

To accurately compare the baseline plaque measurements with those at follow-up within each patient, the carotid bifurcation on both scans were registered using a custom-made semiautomated registration tool (Fig 1). First lumen segmentation was generated by a level-set-based method, initialized with 3 seed points in the CCA, ICA, and ECA.[11] From this lumen segmentation, a CLL was extracted. Then 3 new observer-defined initialization points in, respectively, the CCA, the ICA, and the ECA on the follow-up MDCTA marked the range to be segmented for plaque analysis. Using the bifurcation point (the level at which the CCA lumen separates into the 2 separate lumens of ICA and ECA) as a landmark, the absolute distances along the CLL from this point to the initialization points were calculated and copied to the CLLs of the baseline MDCTA to define the corresponding vessel part of interest on the baseline scan (on axial sections). In this way, adjustments were made for possible differences between the baseline and the follow-up scan in the curvature of the carotid arteries due to elongation or head position. Scan data reconstructed with a B46 kernel were used.

Plaque Analysis

Volume measurements of lumen, vessel wall, and vessel wall components (further defined as plaque and plaque components, respectively) were derived using a custom-made semiautomated plaque analysis method. The lumen segmentation used in registering the vessel range of interest between baseline and follow-up scan was also used here. The outer vessel wall was segmented based on a method using a gentle boost classifier, which had been trained by manually annotated data.[12,13] The lumen segmentations and outer vessel wall segmentations were checked and adjusted manually, where appropriate. The plaque was derived by subtracting the lumen segmentation from the outer vessel wall segmentation.

After segmenting the carotid artery outer vessel wall and lumen, plaque components were differentiated based on HU thresholds. The cut-off value between calcifications and fibrous tissue was set at 130 HU, as used for calcium scoring. The threshold used to differentiate lipid from fibrous tissue was 60 HU, a setting that was previously validated with histology.[5] The volumes of the plaque and plaque components were calculated as the product of the number of pixels in the segmented areas, the pixel size, and the section increment. The proportion of plaque components was calculated as the ratio of the volume of the component to the total plaque volume, multiplied by 100. Figure 2 shows an example of axial sections through a carotid bifurcation at baseline and follow-up and their corresponding plaque segmentations.

Stenosis measurements were performed according to the NASCET criteria. Using 3D software, multiplanar reformats were made and the smallest diameter was measured on axial images perpendicular to the vessel axis.

Reproducibility of Semiautomated Plaque Measurements

Although the procedure was automated for a large part, there were some observer interventions: clicking initialization points for lumen segmentation, clicking initialization points for defining the range for plaque segmentation, and manually adjusting the lumen and outer vessel wall segmentations, if necessary. To assess the intraobserver and interobserver variability of the complete

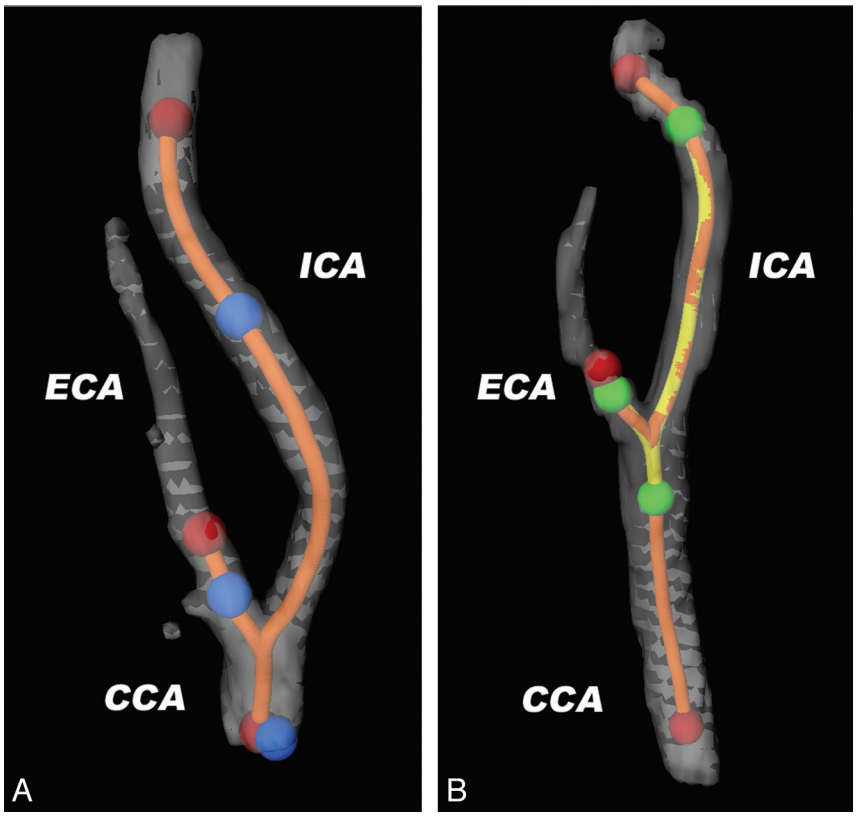

Fig 1. Explanation of the method of semiautomated registration of vessel wall range of interest. 3D reconstructions of the lumen segmentations of a carotid bifurcation at FU (*A*) and at BL (*B*). Lumen segmentation is semiautomatically generated after clicking 3 initialization points in the CCA, the ICA, and the ECA, respectively (*red dots*), separately in both FU and BL datasets. From this lumen segmentation, CLLs are extracted (*orange line*). On the FU CTA, the vessel range containing atherosclerotic plaque is defined by clicking another set of initialization points (*blue dots*). The absolute distances along the CLL between the 3 blue points are measured and copied to the CLL of the BL CTA (*yellow line*), which define the range on axial images to be analyzed by the automated plaque segmentation tool (*green dots*).

method, a subset of 30 carotid arteries was analyzed 2 times by the same observer, with a delay of 3 months, and once by a second observer. This subset was randomly taken from the group of patients without a treated artery, an occluded carotid artery, or poor

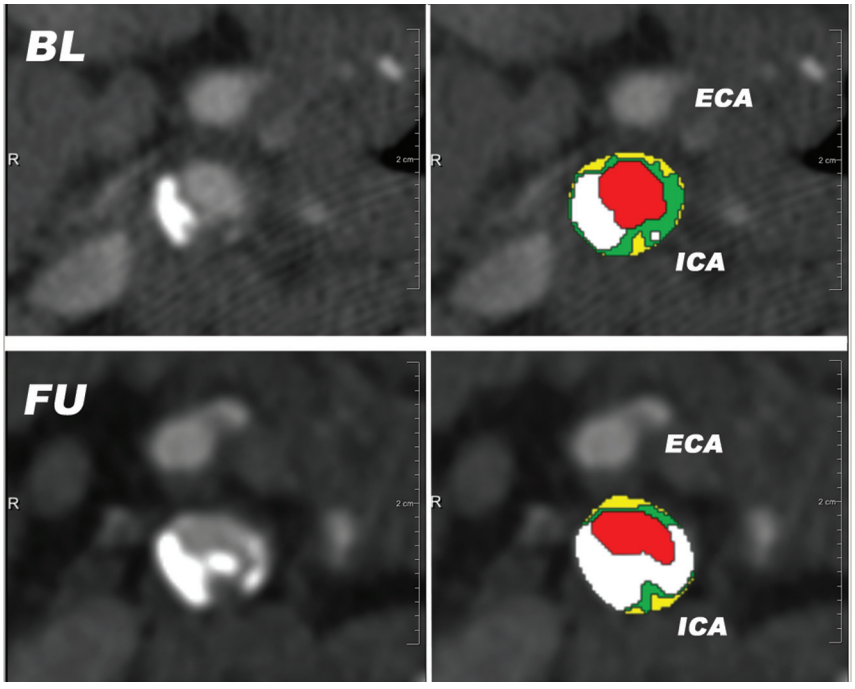

Fig 2. Semiautomatically generated plaque segmentations on matched BL and FU axial MDCTA images just above the level of the carotid bifurcation. The time interval between the scans is 5.8 years; a slight plaque progression with an increase in calcifications is visible. Red = lumen; green = fibrous tissue; yellow = lipid; white = calcification.

Table 1: Baseline patient characteristics

Baseline Patient Characteristics (n = 109)	Value
Age (years; mean ± SD)	62.8 ± 8.5
Male sex (n [%])	70 (64%)
Hypertension (n [%])	76 (70%)
Hypercholesterolemia (n [%])	90 (83%)
Diabetes mellitus (n [%])	11 (10%)
Smoking (current or past; n [%])	87 (80%)
Previous cardiovascular disease (n [%])	19 (17%)
Previous cerebrovascular disease (n [%])	25 (23)%
Symptoms (n [%])	
Amaurosis fugax	18 (17%)
Transient ischemic attack	50 (46%)
Minor stroke	41 (38%)
Use of secondary preventive medication during FU (n [%])	
Cholesterol lowering	98 (90%)
Antihypertensive	80 (73%)
Antidiabetic	17 (16%)
Time delay BL–FU MDCTA (years; mean ± SD)	5.3 ± 0.7

image quality. The intraobserver and interobserver variability are presented as ICC and CoV.

Data Analysis

Plaque volume and plaque component volumes and proportions were measured on both sides in each individual at baseline and follow-up within the registered range of interest. Within each carotid artery, the changes over time of the different plaque measures were derived.

The data are presented as mean ± SD. Total vessel, lumen, plaque, and plaque components are presented as absolute volumes (in mm^3) on baseline and follow-up. Plaque components are also expressed as proportions. A paired t test was used for the analysis of absolute progression from baseline to follow-up.

Temporal changes are expressed as absolute annual change in volume or proportion ([change in volume or proportion/FU time in months]*12), and as a percentage ("relative") annual volume change from baseline (absolute annual change in volume/BL volume). A one-sample t test was used for comparison of "annual change" to 0.

Correlations between percentage annual growth of plaque volume and BL plaque characteristics were described by Pearson correlation coefficient. Correlations between absolute change in plaque component proportion and baseline characteristics were described by Pearson correlation, or by Spearman correlation coefficient, when appropriate. To avoid an induced (spurious) correlation between absolute or percentage annual change in a plaque feature and its baseline value, the mean of the measure at baseline and follow-up was used.[14]

Results

Baseline Characteristics

The clinical information on the 109 included patients is summarized in Table 1. The median time delay between the event and the baseline scan was 11 (IQR 5–21) days and the mean interval between the scans was 5.3 ± 0.7 years. In just a few cases, the degree of stenosis of the artery changed into a higher degree over time (Table 2). Baseline plaque volume was 1100 ± 464 mm^3. The contributions of the different components at baseline were 66.4 ± 7.8%, 28.8 ± 5.4%, and 4.8 ± 6.9% for fibrous tissue, lipid, and calcification, respectively (Table 3). Calcifications were present in 132 carotid arteries (68.4%).

Table 2: Stenosis measurements at baseline and at follow-up as assessed according to the NASCET criteria

	Follow-Up				
Baseline	0–29%	30–49%	50–69%	70–99%	Total
0–29%	160	7	0	1	168
30–49%	1	13	4	0	18
50–69%	0	0	5	1	6
70–99%	0	0	0	1	1
Total	161	20	9	3	193

Atherosclerotic Plaque Growth

Of 193 arteries, 60 (31%) showed decrease in plaque volume (mean difference between BL and FU −119 mm^3, 95% CI, −151 – −86 mm^3), while in 133 (69%), plaque volume increased (mean difference 127 mm^3, 95% CI, 109–146 mm^3). The mean volumes and plaque component proportions at baseline and follow-up for the entire group are summarized in Table 3. There was a significant overall growth in plaque volume of 51 mm^3 (95% CI, 28–74 mm^3). Lumen and total vessel volume also increased significantly over time. Whereas the absolute values of fibrous tissue and lipid did not change significantly, their relative contribution to the plaque volume decreased (−1.5% and −1.8%, respectively, $P < .001$). The proportion of calcification within the plaque increased by 3.3% ($P < .001$).

Annualized Changes in Plaque Measures

Overall, the percentage annual growth of total vessel volume, lumen volume, and plaque volume were 0.63% per year (95% CI, 0.44–0.83), 0.55% per year (95% CI, 0.25–0.85), and 1.16% per year (95% CI, 0.76–1.55), respectively. Absolute annual changes in the proportions of the components were a decrease of 0.26% per year for fibrous tissue (95% CI, −0.41% – −0.10%), a decrease of 0.37% per year for lipid (95% CI, −0.51% – −0.24%), and an increase of 0.64% per year for calcifications (95% CI, 0.54–0.74; all Ps ≤ .001).

Relation Between Plaque Changes and BL Plaque Characteristics

Regression analysis showed no significant correlation between percentage annual plaque growth and plaque volume (P = .196). No correlations were found between percentage annual plaque growth and plaque component proportions at baseline.

The change in calcium proportion was significantly correlated with baseline plaque volume ($r_s = 0.45$, $P < .001$) and calcium proportion ($r_s = 0.68$, $P < .001$). Annual increase in calcium proportion was larger in arteries with baseline plaque volume larger than 975 mm^3 (ie, larger than the median of baseline plaque volume, $n = 96$) compared with arteries with a baseline plaque volume smaller than 975 mm^3 ($n = 97$; 0.88% versus 0.39% per year; $P < .001$). Annual increase in calcium proportion was larger in plaques with a high baseline calcium proportion (>3.9%, median of average calcium proportion on baseline and follow-up, $n = 96$) compared with

Table 3: Baseline and follow-up measurements of plaque volume and plaque components

	BL (± SD)	FU (± SD)	Mean Paired Difference (95% CI)	*P* value[a]
Vessel volume (mm^3)	2575.4 ± 993.6	2657.6 ± 1022.5	82.2 (55.9–108.5)	<0.001
Lumen volume (mm^3)	1475.2 ± 620.2	1506.5 ± 621.9	31.3 (9.8–52.8)	0.005
Plaque volume (mm^3)	1100.2 ± 464.0	1151.1 ± 466.7	50.9 (28.1–73.7)	<0.001
Fibrous volume (mm^3)	712.2 ± 260.7	726.4 ± 262.9	14.2 (−2.4–30.8)	0.094
Lipid volume (mm^3)	318.3 ± 154.1	309.0 ± 134.1	−9.3 (−21.1–2.6)	0.124
Calcium volume (mm^3)	69.7 ± 124.6	115.7 ± 152.9	46.0 (37.6–54.4)	<0.001
Fibrous proportion (%)	66.4 ± 7.8	64.9 ± 9.4	−1.5 (−2.3–−0.7)	<0.001
Lipid proportion (%)	28.8 ± 5.4	27.0 ± 5.9	−1.8 (−2.5–−1.1)	<0.001
Calcium proportion (%)	4.8 ± 6.9	8.1 ± 8.6	3.3 (2.8–3.9)	<0.001

[a] As evaluated with a paired *t* test

Table 4: Intraobserver and interobserver variability ($n = 30$ carotid arteries) of the semiautomatic segmentation method

	Intraobserver				Interobserver			
	Mean ± SD	Diff Obs	ICC	CoV (%)	Mean ± SD	Diff Obs	ICC	CoV (%)
Vessel volume (mm^3)	2606 ± 830	50 ± 244	0.96	9.4	2743 ± 848	323 ± 407	0.84	14.9
Lumen volume (mm^3)	1527 ± 535	−5 ± 152	0.96	10.0	1630 ± 567	201 ± 266	0.85	16.3
Plaque volume (mm^3)	1079 ± 350	55 ± 120	0.93	11.1	1112 ± 334	123 ± 164	0.84	14.7
Fibrous volume (mm^3)	649 ± 178	33 ± 64	0.92	9.9	675 ± 185	86 ± 115	0.76	17.0
Lipid volume (mm^3)	316 ± 114	19 ± 60	0.86	19.0	326 ± 110	39 ± 70	0.78	21.5
Calcium volume (mm^3)	114 ± 120	3 ± 7	1.00	6.5	112 ± 115	2 ± 13	0.99	12.0
Fibrous proportion (%)	61 ± 8	0.5 ± 2.8	0.94	4.6	62 ± 8	0.8 ± 2.7	0.94	4.5
Lipid proportion (%)	29 ± 4	0.1 ± 3.0	0.78	10.4	29 ± 5	0.4 ± 3.0	0.80	10.2
Calcium proportion (%)	9 ± 8	−0.6 ± 1.1	0.99	11.4	9 ± 8	1.2 ± 2.0	0.96	22.0

Note:—Diff Obs indicates difference between observers.

those with a low baseline calcium proportion (<3.9%, $n = 97$; 1.00% versus 0.26% per year; $P < .001$).

Reproducibility of the Method

The ICC for all volume and proportion measures varied between 0.92 and 1.00 for intraobserver reproducibility, except for lipid proportion and lipid volume, which were 0.78 and 0.86, respectively. The ICC for interobserver reproducibility varied between 0.76 and 0.99. The CoVs were good for intraobserver variability, varying between 4.6% and 11.4%, except for lipid volume, which was 19.0%. For interobserver variability, the CoVs were moderate and varied between 4.5% and 22.0% (Table 4).

Discussion

To our knowledge, this is the first in vivo serial CTA study to investigate atherosclerotic carotid plaque progression in humans. This study demonstrates that multidetector CT angiography can be used to quantify atherosclerotic plaque measures in vivo and track changes over time in large study populations.

In 193 carotid arteries, the mean percentage annual growth in plaque volume was 1.2% per year, with a wide range from −5.6% to 10.1% per year. MR imaging has been proven as a reproducible method for plaque quantification,[15-18] and several serial MR imaging studies have been performed for tracking changes in carotid atherosclerosis. In a prospective MR imaging study, Saam et al described a yearly increase of 2.2% in wall area in >50% stenosed carotid arteries.[19] Boussel et al found an annual rate of progression of carotid vessel wall volume of 2.3% per year in arteries with >50% stenosis.[20] In these studies, however, the included arteries had more severe stenosis compared with the arteries included in our study. In another study, a carotid total wall volume increase of 1.2% and 1.8% was found after 16 and 24 months, respectively, in patients who were on statin treatment.[15] These results were comparable with ours. MR imaging studies often use different measures (area or eccentric wall volume) for assessing plaque growth, which leads to another difficulty in comparing our results to those from previous serial in vivo studies. Nevertheless, the growth rate of carotid plaque turns out to be remarkably small and highly variable, a comparable finding across studies. Statin treatment has been shown to induce reduced progression or even regression of plaque burden.[19-25] Approximately 90% of patients in our study were using statins during the follow-up period. Thirty-one percent of our patients showed plaque regression, a number similar to that found in other plaque progression studies in which most patients were on statin therapy.[19,20] Statin treatment might therefore be a reason for the small mean growth in plaque volume.

We did not find any local baseline plaque characteristics significantly associated with plaque volume growth. In contrast, Saam et al found that a normalized wall index >0.64, as a measure of large plaque burden, was associated with a reduced rate of progression in mean wall area.[19]

In this study, we found a change in plaque composition over time: calcification proportion increased, which coincides with a decrease in fibrous and lipid proportion. Larger plaques had a faster increase in calcium proportion compared with smaller plaques, and the more calcified plaques showed a significantly larger annual increase in calcium proportion than the less calcified plaques. Calcified carotid plaques are thought to be more stable compared with noncalcified plaques.[26-28] The results of this longitudinal study therefore suggest that when plaques progress, they finally get a more stable profile. This might also be an effect of the secondary preventive medication that is used by most patients. A few studies reported on the change in composition toward a more stable plaque phenotype in statin-treated patients, by demonstrating a decrease

in lipid content[29,30] and a trend toward more calcium.[30] However, these results should be confirmed in larger randomized trials investigating the influence of statin use on plaque composition.

Glagov et al were the first to report on outward vascular remodeling, showing an increase in total vessel area as an adaptive mechanism to preserve lumen area in response to increasing atherosclerotic disease burden. Luminal narrowing did not occur until the atherosclerotic lesion occupied >40% of the internal elastic lamina area.[1] In our study, including only arteries with mild atherosclerotic disease, we also found an overall increase in total vessel volume following an increase in plaque volume. The changes in plaque burden over time appeared to be too small for lumen to become compromised. This might also explain why a change in degree of stenosis was demonstrated in only a minority of vessels.

One of the major challenges in serial imaging studies on atherosclerotic plaques is the reproducibility of quantitative measures. In our study, we used volume measurements, which have been shown to be more precise than area measurements.[17] Several studies have investigated factors influencing measurement errors. Differences in head positioning is one such factor that can cause the 3D position of the carotid bifurcation to change significantly,[31] thereby causing difficulties in matching corresponding axial cross-sectional images across different time points. So far, registration of carotid arteries has been performed manually using landmarks such as the carotid bifurcation point. In this study, we matched the range of interest in the carotid artery semiautomatically using the distance along the central vessel lumen line, accounting for possible variation in carotid position over time. Further improvement would be achieved if analyses could be performed in sections perpendicular to the central line of the artery.

Semiautomated measurement of plaque volumes might improve reproducibility. When we compare our results, using a semiautomated plaque segmentation method, with the interobserver reproducibility found in a previous study in which plaque segmentation was done manually, interobserver reproducibility improved; CoV for plaque volume was 15% compared with 23%–34% found with the manual segmentation method. De Weert et al demonstrated that their moderate interobserver reproducibility was partly due to the difficulty of defining the exact plaque range; consensus about the segmentation range improved the reproducibility.[7] Therefore, taking a fixed range around the bifurcation to be segmented may further improve interobserver and intraobserver reproducibility of the semiautomated method. Nevertheless, the annual changes in plaque measures are relatively small compared with the current intraobserver variability and, though significant for the whole group, these would not be meaningful for the individual patient.

Our study has some limitations. First, in contrast to MR imaging, MDCTA is not capable of visualizing fibrous cap rupture or intraplaque hemorrhage. Both plaque features are highly associated with plaque rupture and ischemic events.[32-36] Intraplaque hemorrhage has also been associated with an accelerated plaque growth.[35] We have not been able to analyze the influence of this important plaque characteristic on plaque development. On the other hand, HU-based differentiation of plaque components enable serial and automated plaque composition measurements in MDCTA data. Calcifications and changes herein can be accurately measured using MDCTA. Compared with MR imaging datasets, in which multiple sequences are necessary to obtain all plaque information, MDCTA data are more robust and allow minimal observer intervention in the steps toward registration and lumen and vessel wall segmentation. High availability and a quick procedure are advantages of MDCTA that make it a promising tool for serial plaque imaging. With the present CT scanners and precautionary measures, the risks of the potentially harmful radiation exposure and intravenous contrast material can be reduced to a minimum.

Second, we reported on plaque volume, whereas, with MDCTA, we are not able to distinguish atherosclerotic plaque itself from the underlying media. In serial studies, this is of minor importance, because the outcome measure of interest—the difference over time—will merely consist of changes in the plaque itself as the range of interest is registered across BL and FU scans.

No evidence exists for a linear pattern of atherosclerotic plaque growth, and the annual change rate is therefore an artificial measure. However, this study corrects for differences in follow-up time and creates a measure that can be compared across groups and studies.

Further, this study was performed in patients with TIA and stroke who were all on secondary preventive medication. Given the known effects of statins on plaque progression, our results cannot be extrapolated to the asymptomatic population.

Conclusions

The present study shows that MDCTA enables quantification of carotid plaque progression and plaque composition changes in vivo in large patient groups. Carotid atherosclerotic plaque progression seems to be a slow and heterogeneous process. It is unknown yet whether monitoring plaque progression might have future clinical value in risk prediction. Further research should therefore focus on the associations between temporal plaque changes found with serial imaging and (recurrent) ischemic cerebrovascular events.

Disclosures: Marjon van Gils—*RELATED: Support for Travel to Meetings for the Study or Other Purposes:* Netherlands Hearth Foundation. Wiro Niessen—*RELATED: Grant:* Dutch Science Foundation; *UNRELATED: Grants/Grants Pending:* Dutch Science Foundation. Aad van der Lugt—*UNRELATED: Payment for Lectures (including service on speakers bureaus):* E Healthcare.* (**Money paid to institution.*)

References

1. Glagov S, Weisenberg E, Zarins CK, et al. **Compensatory enlargement of human atherosclerotic coronary arteries.** *N Engl J Med* 1987;316:1371–75
2. Naghavi M, Libby P, Falk E, et al. **From vulnerable plaque to vulnerable patient: a call for new definitions and risk assessment strategies: Part I.** *Circulation* 2003;108:1664–72
3. Underhill HR, Yuan C, Yarnykh VL, et al. **Predictors of surface disruption with MR imaging in asymptomatic carotid artery stenosis.** *AJNR Am J Neuroradiol* 2010;31:487–93
4. Finn AV, Nakano M, Narula J, et al. **Concept of vulnerable/unstable plaque.** *Arterioscler Thromb Vasc Biol* 2010;30:1282–92
5. de Weert TT, Ouhlous M, Meijering E, et al. **In vivo characterization and quantification of atherosclerotic carotid plaque components with multidetector computed tomography and histopathological correlation.** *Arterioscler Thromb Vasc Biol* 2006;26:2366–72

6. Wintermark M, Jawadi SS, Rapp JH, et al. **High-resolution CT imaging of carotid artery atherosclerotic plaques.** *AJNR Am J Neuroradiol* 2008;29:875–82
7. de Weert TT, de Monye C, Meijering E, et al. **Assessment of atherosclerotic carotid plaque volume with multidetector computed tomography angiography.** *Int J Cardiovasc Imaging* 2008;24:751–59
8. Homburg PJ, Rozie S, van Gils MJ, et al. **Atherosclerotic plaque ulceration in the symptomatic internal carotid artery is associated with nonlacunar ischemic stroke.** *Stroke* 2010;41:1151–56
9. de Weert TT, Ouhlous M, Zondervan PE, et al. **In vitro characterization of atherosclerotic carotid plaque with multidetector computed tomography and histopathological correlation.** *Eur Radiol* 2005;15:1906–14
10. Nickoloff EL. **Measurement of the PSF for a CT scanner: appropriate wire diameter and pixel size.** *Phys Med Biol* 1988;33:149–55
11. Manniesing R, Schaap M, Rozie S, et al. **Robust CTA lumen segmentation of the atherosclerotic carotid artery bifurcation in a large patient population.** *Med Image Anal* 2010;14:759–69
12. Vukadinovic D, Rozie S, van Gils M, et al. **Automated versus manual segmentation of atherosclerotic carotid plaque volume and components in CTA: associations with cardiovascular risk factors.** *Int J Cardiovasc Imaging* 2012;28:877–87
13. Vukadinovic D, van Walsum T, Manniesing R, et al. **Segmentation of the outer vessel wall of the common carotid artery in CTA.** *IEEE Trans Med Imaging* 2010;29:65–76
14. Tu YK, Baelum V, Gilthorpe MS. **The problem of analysing the relationship between change and initial value in oral health research.** *Eur J Oral Sci* 2005;113:271–78
15. Adams GJ, Greene J, Vick GW 3rd, et al. **Tracking regression and progression of atherosclerosis in human carotid arteries using high-resolution magnetic resonance imaging.** *Magn Reson Imaging* 2004;22:1249–58
16. Kang X, Polissar NL, Han C, et al. **Analysis of the measurement precision of arterial lumen and wall areas using high-resolution MRI.** *Magn Reson Med* 2000;44:968–72
17. Saam T, Kerwin WS, Chu B, et al. **Sample size calculation for clinical trials using magnetic resonance imaging for the quantitative assessment of carotid atherosclerosis.** *J Cardiovasc Magn Reson* 2005;7:799–808
18. Saam T, Hatsukami TS, Yarnykh VL, et al. **Reader and platform reproducibility for quantitative assessment of carotid atherosclerotic plaque using 1.5T Siemens, Philips, and General Electric scanners.** *J Magn Reson Imaging* 2007;26:344–52
19. Saam T, Yuan C, Chu B, et al. **Predictors of carotid atherosclerotic plaque progression as measured by noninvasive magnetic resonance imaging.** *Atherosclerosis* 2007;194:e34–42
20. Boussel L, Arora S, Rapp J, et al. **Atherosclerotic plaque progression in carotid arteries: monitoring with high-spatial-resolution MR imaging–multicenter trial.** *Radiology* 2009;252:789–96
21. Corti R, Fayad ZA, Fuster V, et al. **Effects of lipid-lowering by simvastatin on human atherosclerotic lesions: a longitudinal study by high-resolution, noninvasive magnetic resonance imaging.** *Circulation* 2001;104:249–52
22. Corti R, Fuster V, Fayad ZA, et al. **Lipid lowering by simvastatin induces regression of human atherosclerotic lesions: two years' follow-up by high-resolution noninvasive magnetic resonance imaging.** *Circulation* 2002;106:2884–87
23. Yonemura A, Momiyama Y, Fayad ZA, et al. **Effect of lipid-lowering therapy with atorvastatin on atherosclerotic aortic plaques: a 2-year follow-up by noninvasive MRI.** *Eur J Cardiovasc Prev Rehabil* 2009;16:222–28
24. Nissen SE, Nicholls SJ, Sipahi I, et al. **Effect of very high-intensity statin therapy on regression of coronary atherosclerosis: the ASTEROID trial.** *JAMA* 2006;295:1556–65
25. Underhill HR, Yuan C, Yarnykh VL, et al. **Arterial remodeling in [corrected] subclinical carotid artery disease.** *JACC Cardiovasc Imaging* 2009;2:1381–89
26. Kwee RM. **Systematic review on the association between calcification in carotid plaques and clinical ischemic symptoms.** *J Vasc Surg* 2010;51:1015–25
27. Nandalur KR, Hardie AD, Raghavan P, et al. **Composition of the stable carotid plaque: insights from a multidetector computed tomography study of plaque volume.** *Stroke* 2007;38:935–40
28. Shaalan WE, Cheng H, Gewertz B, et al. **Degree of carotid plaque calcification in relation to symptomatic outcome and plaque inflammation.** *J Vasc Surg* 2004;40:262–69
29. Underhill HR, Yuan C, Zhao XQ, et al. **Effect of rosuvastatin therapy on carotid plaque morphology and composition in moderately hypercholesterolemic patients: a high-resolution magnetic resonance imaging trial.** *Am Heart J* 2008;155:584 e581–88
30. Zhao XQ, Yuan C, Hatsukami TS, et al. **Effects of prolonged intensive lipid-lowering therapy on the characteristics of carotid atherosclerotic plaques in vivo by MRI: a case-control study.** *Arterioscler Thromb Vasc Biol* 2001;21:1623–29
31. Aristokleous N, Seimenis I, Papaharilaou Y, et al. **Effect of posture change on the geometric features of the healthy carotid bifurcation.** *IEEE Trans Inf Technol Biomed* 2011;15:148–54
32. Altaf N, MacSweeney ST, Gladman J, et al. **Carotid intraplaque hemorrhage predicts recurrent symptoms in patients with high-grade carotid stenosis.** *Stroke* 2007;38:1633–35
33. Hatsukami TS, Ross R, Polissar NL, et al. **Visualization of fibrous cap thickness and rupture in human atherosclerotic carotid plaque in vivo with high-resolution magnetic resonance imaging.** *Circulation* 2000;102:959–64
34. Yuan C, Zhang SX, Polissar NL, et al. **Identification of fibrous cap rupture with magnetic resonance imaging is highly associated with recent transient ischemic attack or stroke.** *Circulation* 2002;105:181–85
35. Takaya N, Yuan C, Chu B, et al. **Presence of intraplaque hemorrhage stimulates progression of carotid atherosclerotic plaques: a high-resolution magnetic resonance imaging study.** *Circulation* 2005;111:2768–75
36. Takaya N, Yuan C, Chu B, et al. **Association between carotid plaque characteristics and subsequent ischemic cerebrovascular events: a prospective assessment with MRI–initial results.** *Stroke* 2006;37:818–23